Performance of reinforcing steel in concrete containing silica fume and blast-furnace slag ponded with sodium-chloride solution

Gu, P.; Beaudoin, J. J.; Zhang, M. H.; Malhotra, V. M.

Publisher's version / Version de l'éditeur:

ACI Materials Journal, 97, 3, pp. 254-261, 2000-06-01

Performance of reinforcing steel in concrete containing silica fume and blast-furnace slag ponded with sodium-chloride solution

NRCC-42677

Gu, P.; Beaudoin, J.J.; Zhang, M.H.; Malhotra, V.M.

June 2000

A version of this document is published in / Une version de ce document se trouve dans:
CI Materials Journal, 97, (3), pp. 254-261, June 01, 2000

ACI MATERIALS JOURNAL TECHNICAL PAPER
Title no. 97-M31

Performance of Reinforcing Steel in Concrete Containing Silica Fume and Blast-Furnace Slag Ponded with Sodium Chloride Solution

by Ping Gu, J. J. Beaudoin, Min-Hong Zhang, and V. M. Malhotra

This paper describes the performance of steel reinforcement in concrete slabs that were ponded with a 3.4% sodium chloride solution for a period of 6 months. The concrete slabs were cast using portland cement concrete with and without silica fume and blast-furnace slag. The concrete cover to steel reinforcing bars ranged from 13 to 76 mm. The concrete resistance to chloride ion penetration was determined according to ASTM C 1202. The corrosion resistance of the steel reinforcing bars was determined using half-cell potential, linear polarization, and AC impedance techniques. The test results showed that both the silica fume and slag concretes exhibited very low penetrability to chloride ions, with the value of charge passed being less than 1000 coulombs. All control concretes had the value of charge passed greater than 1000 coulombs, regardless of the water-cement ratio (w/c). There was no significant corrosion of the reinforcing steel in the silica fume, slag, and control portland cement concrete with water-cementitious materials ratio (w/cm) of 0.32 after 6 months of ponding with a 3.4% sodium chloride solution. Significant corrosion rates were observed for the reinforcing steel embedded in control portland cement concrete with w/c ≥ 0.43. As expected, the poorest performance was of the control concrete with a w/c of 0.76, where the corrosion of reinforcing steel was detected, even with a 51 mm concrete cover. There was a good correlation among the test results obtained using the half-cell potential, linear polarization, and AC impedance techniques.

Keywords: blast-furnace slag; portland cement concrete; reinforcement; silica fume; slab; water-cement ratio

INTRODUCTION

It is well documented that portland cement concrete incorporating supplementary cementing materials such as fly ash, blast-furnace slag, and silica fume develops excellent mechanical properties and long-term durability characteristics.[1] In addition, the use of these materials is environmentally friendly because they partially replace portland cement, the production of which releases significant amounts of CO_2 to the environment.[2] Published data on the silica fume and slag concretes suggest that they reduce the chloride ion penetration into concrete.[3-5] For this reason, a superior corrosion resistance of the steel reinforcement in these concretes is expected.[6-8]

This paper reports the results of an investigation undertaken to determine the relative performance of steel reinforcing bars embedded at various cover depths in portland cement concrete slabs incorporating silica fume or blast-furnace slag, and ponded with a 3.4% sodium chloride solution for up to 6 months. The resistance of the concrete to the penetration of chloride ions was determined using ASTM C 1202. The performance of the reinforcing steel bars was evaluated using various DC electrochemical techniques (half-cell potential and linear polarization) and an AC technique (AC impedance).

SCOPE

Six large concrete slabs, 833 x 600 x 153 mm in size, were cast. These consisted of four control portland cement concrete slabs with water-cement ratios (*w/c*) ranging from 0.32 to 0.76, and two slabs made with concrete incorporating 10% silica fume and 55% blast-furnace slag with water-cementitious materials ratios (*w/cm*) of 0.32 and 0.33, respectively. The AC impedance, linear polarization, and half-cell potential techniques were applied to monitor the corrosion progression of the steel reinforcement in the concrete.

EXPERIMENTAL

Materials

Cement—An ASTM Type I portland cement was used. Its physical properties and chemical composition are given in Table 1.

Silica fume—A dry, uncompacted silica fume from the production of silicon metal was used. It contains 93.7% SiO_2, and has a specific surface of 26.1 m^2/g, determined by the nitrogen adsorption method. The detailed chemical composition and

Table 1—Physical properties and chemical analysis of the cement, silica fume, and slag

Physical Tests	Cement ASTM Type I	Silica Fume	Slag
Specific gravity	3.15	2.16	2.99
Fineness			
-passing 45μm, %	87.9	98.9	96.9
-specific surface, Blaine, m^2/kg	388	-	449
-nitrogen absorption, m^2/g	-	26.1	-
Compressive strength of 51-mm cubes, MPa			
-7-day	33.5	-	-
-28-day	39.7	-	-
Water requirement, %	-	111.6	97.1
Pozzolanic Activity Index, %			
-7-day	-	128.8	-
Slag activity index, %			
- 7-day	-	-	77.6
- 28-day	-	-	102.8
Chemical Analyses, %			
Silicon dioxide (SiO_2)	20.6	93.7	36.6
Aluminum oxide (Al_2O_3)	4.0	0.2	9.8
Ferric oxide (Fe_2O_3)	3.1	0.3	0.5
Calcium oxide (CaO)	62.8	0.4	35.1
Magnesium oxide (MgO)	2.6	0.5	13.0
Sodium oxide (Na_2O)	-	0.2	0.4
Potassium oxide (K_2O)	-	1.2	0.5
Equivalent alkali ($Na_2O+0.658K_2O$)	0.8	1.0	0.7
Phosphorous oxide (P_2O_5)	-	0.1	-
Titanium oxide (TiO_2)	-	0.01	-
Sulphur trioxide (SO_3)	3.1	0.3	3.8
Loss on ignition	1.8	2.7	1.4
Bogue Potential Compound Composition			
Tricalcium silicate C_3S	59.3	-	-
Dicalcium silicate C_2S	14.4	-	-
Tricalcium aluminate C_3A	5.3	-	-
Tetracalcium aluminoferrite C_4AF	9.3	-	-

ACI Materials Journal, V. 97, No. 3, May-June 2000.
MS No. 99-011 received February 25, 1999, and reviewed under Institute publication policies. Pertinent discussion will be published in the March-April 2001 *ACI Materials Journal* if received by December 1, 2000.

Table 5—Compressive strength and resistance of hardened concrete to chloride ion penetration

Mix No.	Type of SCM*	SCM* content, %	W/C+SCM	Unit weight, kg/m³	Compressive strength, MPa				Resistance to Chloride-ion Penetration, coulombs
					7d	28d	91d	365d	28d
N7	Silica fume	10	0.32	2402	56.8	64.3	65.3	75.5	235
N8	BFS	55	0.33	2481	38.6	45.6	51.4	54.9	670
N3	-	-	0.32	2450	51.7	61.1	67.1	78.6	1730
N5	-	-	0.43	2331	35.4	37.7	41.0	48.2	3970
N6	-	-	0.55	2343	26.5	31.0	33.5	35.7	5250
N4	-	-	0.76	2304	14.6	18.4	20.7	21.7	5970

* Supplementary cementing materials.

Table 6—Chloride ion penetrability based on charge passed (ASTM C 1202 guidelines)

Charge passed (coulombs)	Chloride-Ion Penetrability
>4,000	High
2,000-4,000	Moderate
1,000-2,000	Low
100-1,000	Very Low
<100	Negligible

Table 7—General guidelines for half-cell potential data interpretation

Half-cell potential reading, vs. Cu/CuSO₄ (ASTM C 876)	Half-cell potential reading, vs. Hg/HgCl₂ (used in the experiment)	Corrosion Activity
less negative than –200 mV	less negative than –128 mV	90% probability of no corrosion
Between -200 mV and –350 mV	Between -128 mV and -278 mV	Corrosion of the embedded steel is uncertain
more negative than –350 mV	more negative than –278 mV	90% probability of corrosion

* Standard potential of $Cu/CuSo_4$ and $Hg/HgCl_2$ is 340 and 268 mV versus that of hydrogen standard electrode, respectively. Difference of two reference electrodes is 72 mV.

results presented are the averages from two concrete specimens (Table 5). The ASTM guidelines concerning the chloride ion penetrability are given in Table 6.

Chloride ponding test—One reinforced concrete slab, 833 x 600 x 153 mm in size (Fig. 1), was cast from each concrete mixture, and consolidated using an internal vibrator. Four pairs of reinforcing bars were embedded in each concrete slab, with concrete covers ranging from 13 to 76 mm, as shown in Fig. 1. The slabs were cured under wet burlap for 7 days, and then exposed to the laboratory air for approximately 50 days. The top surface of the slabs was ponded with a 3.4% sodium chloride solution, and the corrosion progression of the steel reinforcement was assessed using half-cell potential, linear polarization, and AC impedance techniques after 2 and 6 months of the ponding. The data presented are the averages of the tests on two reinforcing bars at each concrete cover thickness.

ASSESSMENT TECHNIQUES FOR CORROSION OF STEEL REINFORCEMENT

Half-cell potential

The half-cell potential is an indication of the relative probability of corrosion activity, and was determined according to ASTM C 876, with minor difference. In the experiment, a $Hg/HgCl_2$ electrode (calomel electrode) was used instead of a $Cu/CuSO_4$ electrode, as specified in ASTM C 876. The standard potential of saturated $Cu/CuSO_4$ and $Hg/HgCl_2$ is 340 and 268 mV versus that of standard hydrogen electrode (SHE), respectively, and the difference of the two reference electrodes

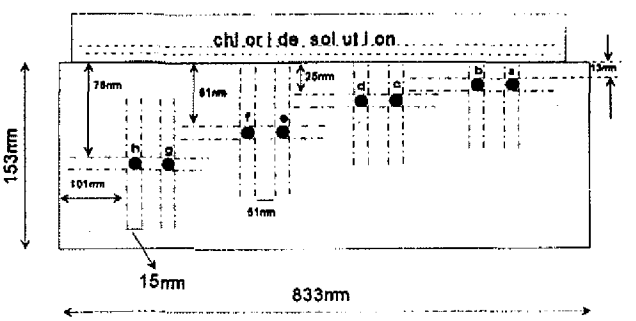

Fig. 1—Reinforcing steel layout of reinforced concrete test slabs.

is 72 mV. The guidelines described in ASTM C 876 provide general principles for the evaluation of the reinforcing steel corrosion in concrete (Table 7).

Linear polarization technique

This method involves the application of a slow potential scan of ±20 mV close to the corrosion potential Φ_{corr} and the recording of the polarization current I. The polarization resistance R_p of the reinforcing steel is defined as the slope of a potential current density plot at the corrosion potential

$$R_p = \left(\frac{\Delta V}{\Delta I}\right)_{\Phi corr} \quad (1)$$

where ΔV and ΔI are applied potential and current response, respectively. The corrosion current density is calculated from

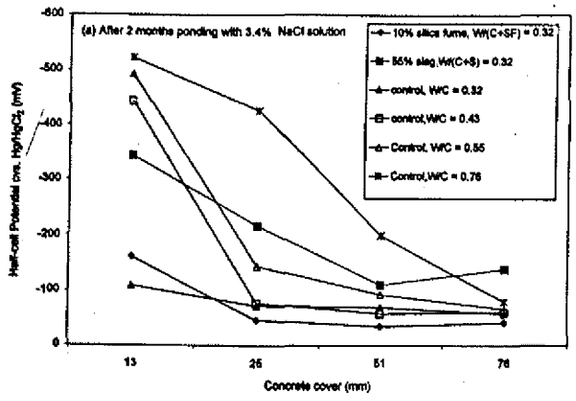

Fig. 2—Half-cell potentials of silica fume and BFS concrete slabs (N7 and N8) and four controls (N3 and N6) measured after: (a) 2 months; and (b) 6 months of sodium chloride solution ponding.

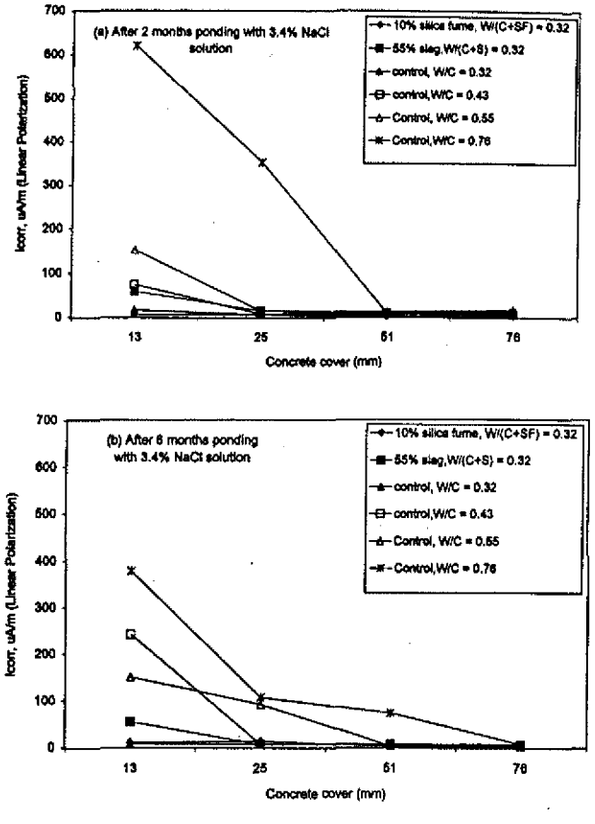

Fig. 3—Corrosion rate I_{corr}, obtained by linear polarization technique applied to silica fume and BFS concrete slabs (N7 and N8) and four control slabs (N3 to N6) measured after: (a) 2 months; and (b) 6 months of sodium chloride solution ponding.†

† The I_{corr} values for the reinforcing bars with 13 and 25 mm concrete covers of the control concrete slab with a w/c of 0.76 obtained after 2 months of ponding with the sodium chloride solution were higher than those obtained after 6 months of ponding with the solution. This behavior may be attributed to the accumulation of corrosion products. When chloride induced corrosion takes place on the surface of the steel reinforcement, I_{corr} could be high initially as the electrochemical reation ($Fe = Fe^{+2} + 2e^-$) is favored to the oxidation of Fe. However, the reaction will decline as the Fe^{+2} ion concentration increases leading to an increase of the reverse reation (Fe reduction) and decrease of the I_{corr}

the Stern-Geary equation[9]

$$I_{corr} = \frac{B}{R_p} \quad \text{and} \quad B = \frac{\beta_a \beta_c}{2.303(\beta_a + \beta_c)} \qquad (2)$$

where B is the so-called Stern-Geary constant that can be determined by a mass loss experiment, and β_a and β_c are the Tafel slopes for the anodic and cathodic reactions, respectively. Values of B between 13 and 52 mV are often used. For example, 50 mV was used by John et al.,[10] and 35 mV by Wenger and Galland.[11] Andrade[12] suggested a value of 26 or 52 mV to be utilized in the calculation for the carbon steel in the active and passive stages, respectively. The value of B = 26 mV is estimated, assuming β_a and β_c as 120 mV/decade.

The linear polarization experiments were performed at a scan rate of 0.1 mV/s (ASTM G 59 recommends a scan rate of < 0.1667 mV/s). They were initiated at 20 mV more negative than the corrosion potential, and terminated at 20 mV more negative than the corrosion potential. The IR drop can be corrected for ($R_p = \Delta V / I_{measured} - R_c$) using the concrete resistance R_c obtained from AC impedance measurement. In this study, however, the correction was insignificant due to the small current. The electrochemical measurements were made using a potentiostat, and the $Hg/HgCl_2$ (calomel) reference electrode was used.

A guideline for the estimation of corrosion extent using corrosion current is given in Table 8.[13]

AC impedance technique

The use of the AC impedance technique in reinforced concrete corrosion studies was first started in the 1980s.[10] This technique has since been used by an increasing number of researchers for the determination of corrosion current in the reinforcing steel in concrete.[14-21] Interpretation of an impedance spectrum, however, is difficult due to the complexity of the reinforced concrete system. The equivalent circuit fitting is commonly applied to analyze the impedance spectra. The accuracy of such an approach relies strongly on how the electrical components are selected, and the extent to which they represent the microstructure of the steel/concrete interface.[15,17,21] More details about this technique are given in the Appendix.*

The AC impedance measurements were carried out using a SI 1255 HF frequency response analyzer and a SI 1286 electrical interface. A small sinusoidal voltage signal of 30 mV was applied over the range of frequencies 75 kHz to 0.05 Hz. The current response caused by the voltage perturbation was measured as well as the phase shift of the current and voltage characteristics. A three-electrode configuration was used. A large

*The Appendix is available in xerographic or similar form from ACI headquarters, where it will be kept permanently on file, at a charge equal to the cost of reproduction plus handling at the time of request.

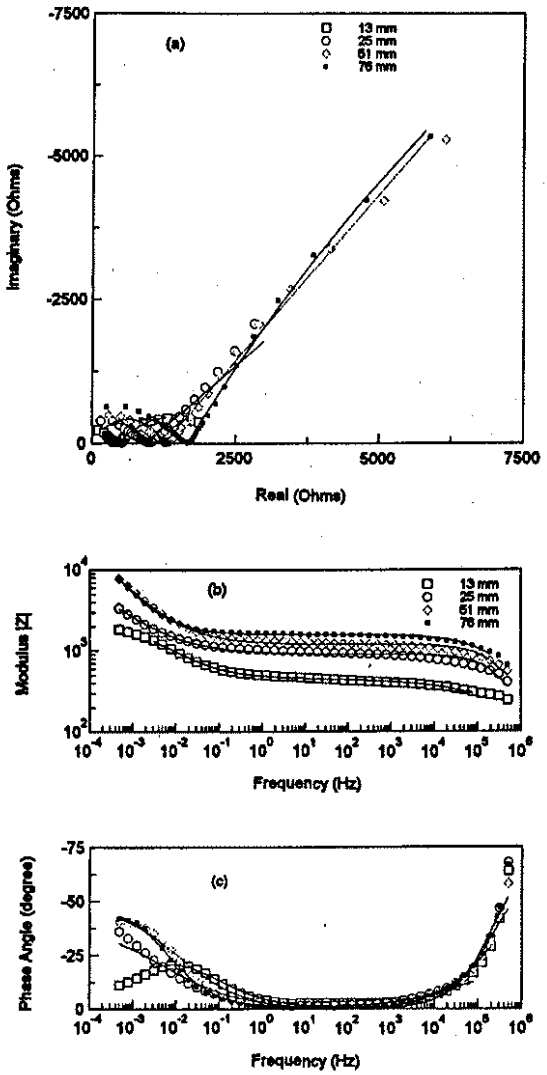

Fig. 4—Typical example (recorded from slab N7 after two months of ponding with 3.4% sodium chloride solution) of experimental data fitting using electrical equivalent circuit (Fig. A1 in Appendix) is presented in plots of: (a) real versus imaginary; (b) log (modulus) versus log (frequency); and (c) phase angle versus log (frequency).*

counter electrode that covered the entire length of the steel reinforcement was applied to the concrete surface to obtain even polarization. The corrosion rate is normally expressed by $\mu A/cm^2$ or $\mu A/m^2$. As it is difficult to determine the surface area of the reinforcing bars accurately, it may be more appropriate to use the unit length instead of unit area to present the data of the reinforcement corrosion rate. Therefore, a unit of $\mu A/m$ is used in the following discussion.

The detailed determination procedure is given elsewhere.[22] The corrosion current density was calculated by knowing the polarization resistance R_p and using the Stern-Geary equation (Eq. (2)).[22]

RESULTS AND DISCUSSION

Resistance to chloride ion penetration (ASTM C 1202)

The silica fume and slag concrete had higher resistance to chloride ion penetration than the control concrete, as indicated by ASTM C 1202 (Table 5). The accumulated charge passed was 235 and 670 coulombs for the silica fume and slag concretes, respectively. These values were much lower than 1730 Coulombs for the control concrete with a w/c of 0.32. According to ASTM C 1202, concrete with a charge value of less than 1000 Coulombs is considered to have an excellent resistance to the penetration of chloride ions.

Half-cell potential of steel reinforcement in concrete slabs

The ASTM C 876 guidelines for the evaluation of the reinforcing steel corrosion in concrete suggest that, in general, the more negative potential readings are associated with the higher probability of the reinforcing steel corrosion. This approximation is reasonably accurate when chloride ions are present.

Figure 2(a) and (b) show the half-cell potential versus the thickness of concrete cover for the silica fume and slag concrete slabs (N7 and N8), and the four control concrete slabs (N3 to N6) after 2 and 6 months of ponding in the sodium chloride solution. Most of the half-cell potential readings for the reinforcing steel bars embedded in the silica fume concrete and the control concrete with a w/c of 0.32 were relatively noble, with half-cell potentials less negative than -128 mV (versus SCE) after 6 months. These readings indicate low probability of the reinforcing steel corrosion. For the slag concrete slab, the half-cell potentials of the first two reinforcing steel bars (with concrete cover of 13 mm) were more negative than -300 mV (versus SCE). After 6 months of ponding, both reinforcing steel bars with 13 and 25 mm concrete covers in slab N4 (w/c = 0.76) showed the highest negative potentials (-450 to -550 mV versus SCE); similarly, high negative potentials were also observed for the reinforcing steel bars with 13 mm cover in slabs N5 (w/c = 0.43) and N6 (w/c = 0.55). After 6 months of the chloride ponding, the reinforcing steel bars with 25 mm concrete cover in control concrete slab N6 (w/c = 0.55) revealed a potential value of -321 mV versus SCE, indicating a high probability of corrosion. The reinforcing steel bars with 51 mm concrete cover in slab N4 (w/c = 0.76) had a potential value of -226 mV (versus SCE) after 6 months of the chloride ponding, which indicated that the corrosion of the corresponding steel bars is uncertain.

Corrosion current determination using linear polarization technique

Figure 3(a) and (b) illustrate the corrosion rate I_{corr} obtained by the linear polarization technique for the silica fume and slag concrete slabs (N7 and N8) and the four control portland cement concrete slabs (N3 to N6) after 2 and 6 months of ponding with the chloride solution.

The values of I_{corr} for all the reinforcing bars in the silica fume concrete and control concrete with a w/c of 0.32 were less than 15 $\mu A/m$, regardless of the thickness of the concrete cover. This revealed that the silica fume concrete provided good protection against chloride ion penetration. A corrosion current of about 55 $\mu A/m$ was observed for the reinforcing bars in the slag concrete with 13 mm cover after 6 months of ponding.

In contrast, the I_{corr} values were much higher for the reinforcing bars with 13 mm concrete cover in the control concrete slab with w/c of 0.76, 0.55, and 0.43 after 6 months of ponding, compared with those in the silica fume and slag concrete slabs, and in the control concrete slab with a w/c of 0.32 (Fig. 3(a)). The progress of corrosion of the steel reinforcing bars was clearly observed in the concrete slabs with w/c of 0.55 and 0.76. The reinforcing bars with 51 mm concrete cover in Slab N4 (w/c = 0.76) and with 25 mm cover in concrete Slab N6 (w/c = 0.55) showed a significant increase in their corrosion current from 2 to 6 months of ponding with the chloride solution (Fig. 3(a) and (b)).

*The Appendix is available in xerographic or similar form from ACI headquarters, where it will be kept permanently on file, at a charge equal to the cost of reproduction plus handling at the time of request.

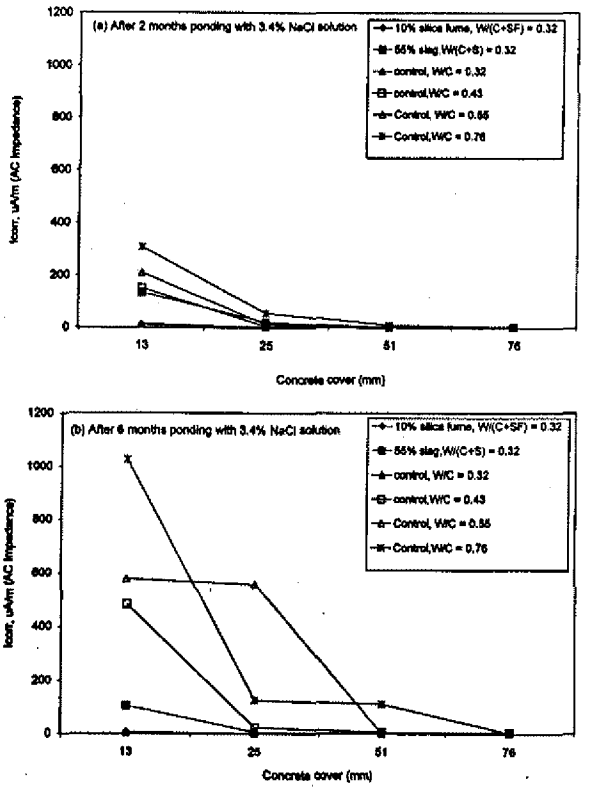

Fig. 5— Corrosion rate I_{corr} obtained by AC impedance applied to silica fume and BFA concrete slabs (N7 and N8) and four control slabs (N3 and N6) measured after (a) 2 months; and (b) 6 months of sodium chloride solution ponding.

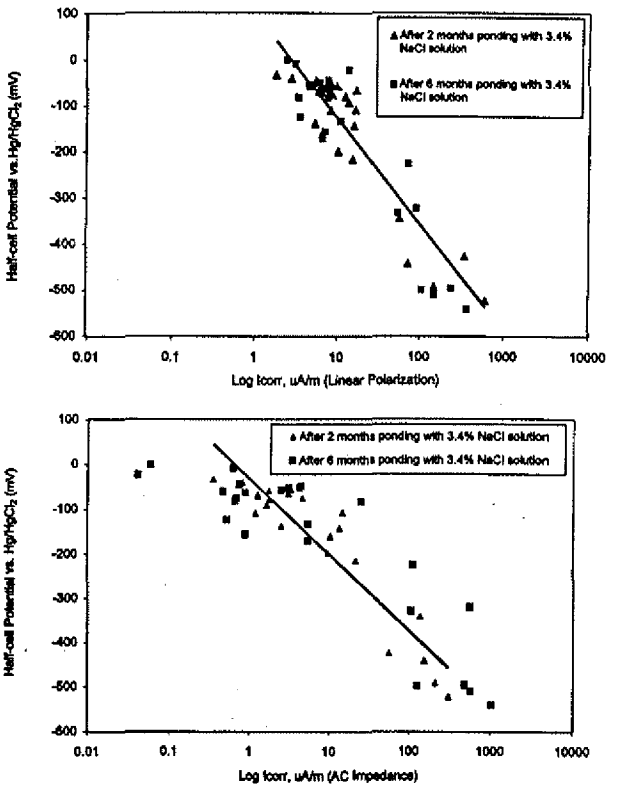

Fig. 6—Plots of half-cell potential versus logarithmic corrosion rate determined by: (a) linear polarization technique; and (b) AC impedance technique.

AC Impedance measurement and corrosion current determination

The corrosion current in the steel reinforcing bars in the six slabs was determined using the AC impedance technique. An equivalent circuit fitting of the experimental impedance spectra procedure was applied to estimate the value of the polarization resistance R_p. A typical example of the experimental data fitting using the electrical equivalent circuit models, as described in Fig. A1 (Appendix),* is given in Fig. 4. Results are presented in the plots of real versus imaginary (Fig. 4(a)), and Bode plots—for example, log [modulus] versus log [frequency] (Fig. 4(b)), and phase angle versus log [frequency] (Fig. 4(c)). The symbols represent the experimental data, and the solid lines represent the computer fitting results. Two partial arcs were observed in the real versus imaginary plot (or Nyquist plot). These arcs are associated with the concrete matrix and the steel surface corrosion process (the steel-concrete interface film was not observed). Very good agreement was obtained between the experimental data and the computer-generated values, as can be seen in Fig. 4(a) to (c). The values of R_p were determined using the best-fit approach. Figure 5(a) and (b) show the corrosion current I_{corr} of the silica fume and slag concrete slabs (N7 and N8) and the four control portland cement concrete slabs (N3 to N6) after 2 and 6 months ponding with the chloride solution, respectively. The values of I_{corr} were less than 20 μA/m for all the steel reinforcing bars embedded in the silica fume concrete and control concrete with a w/c of 0.32 after 6 months. The steel reinforcing bar with 13 mm concrete cover in the slag concrete had a relatively higher I_{corr} value than that of the silica fume concrete slab after both 2 and 6 months of the ponding with 3.4% NaCl. The values of I_{corr} for all the reinforcing bars with 13 mm cover in concrete slabs with $w/c \geq 0.43$, however, were significantly higher after both 2 and 6 months (> 150 μA/m after 2 months).

*The Appendix is available in xerographic or similar form from ACI headquarters, where it will be kept permanently on file, at a charge equal to the cost of reproduction plus handling at the time of request.

Comparison of results obtained by three electrochemical techniques

As on page 257 the results obtained by the half-cell potential, linear polarization, and AC impedance techniques are in good agreement. More negative half-cell potential readings were associated with larger corrosion current determined by both the AC impedance and linear polarization techniques.

The plots of the half-cell potential versus logarithmic corrosion rate determined by the linear polarization and AC impedance techniques are given in Fig. 6(a) and (b), respectively. A linear trend for the potential log (I_{corr}) relation appears to exist. The I_{corr} data obtained by the linear polarization method exhibits less scattering than those obtained by the AC impedance. In fact, the linear relationship between corrosion potential and log(I_{corr}) exists theoretically in the chloride-induced corrosion.[23]

A comparison of the I_{corr} values obtained by the linear polarization and AC impedance techniques in a log-log plot is presented in Fig. 7. A solid reference line is applied to indicate a linear trend between the two measurements. It appears that both techniques are in a relatively good agreement with respect to I_{corr} values when the reinforcing steel is under active corrosion. The AC impedance technique, however, tends to give lower I_{corr} values when the reinforcing steel is in a passive state.

Corrosion of steel reinforcement in concrete

The concrete cover is a physical barrier that impedes the chloride ion penetration, thus protecting the reinforcing steel from corrosion. Good quality and proper depth of concrete

Table 8—Guideline for estimation of corrosion extent using I_{corr}

Corrosion Current Density ($\mu A/cm^2$)*	Corrosion rate ($\mu A/m$)**	Extent of Corrosion
$I_{corr} < 0.1$	<47	P: passive condition
$0.1 < I_{corr} < 0.5$	47< C.R.< 235	L: low to moderate corrosion
$0.5 < I_{corr} < 1$	235< C.R.< 470	M: moderate to high corrosion
$I_{corr} > 1$	>470	H: high corrosion

* From Reference 23.
**1 m of No. 5 reinforcing bar (diameter of 15 mm) has geometrical area of 470 cm^2.

Table 9(a)—Probability of corrosion after 6 months evaluated by half-cell potential method

No.	Concrete mixture	13mm	25mm	51mm	76mm
N7	Concrete incorporating 10% silica fume, w/(c+sf) = 0.32	mid	Low	Low	Low
N8	Concrete incorporating 55% slag, w/(c+s) = 0.32	High	Mid	Mid	Low
N3	Portland cement concrete (control), w/c= 0.32	Low	Low	Low	Low
N5	Portland cement concrete (control), w/c= 0.43	High	Low	Low	Low
N6	Portland cement concrete (control), w/c= 0.55	High	High	Low	Low
N4	Portland cement concrete (control), w/c= 0.76	High	High	Mid	Low

Note: Low = half-cell potential less negative than -128 mV, indicating a 90% probability of no corrosion; Mid = half-cell potential between -128 and -278 mV, indicating that corrosion of embedded steel is uncertain; and High = half-cell potential more negative than -278 mV, indicating 90% probability of corrosion.

Table 9(b)—Severity of corrosion after 6 months evaluated by linear polarization technique

No.	Concrete mixture	13mm	25mm	51mm	76mm
N7	Concrete incorporating 10% silica fume, w/(c+sf) = 0.32	P	P	P	P
N8	Concrete incorporating 55% slag, w/(c+s) = 0.32	L	P	P	P
N3	Portland cement concrete (control), w/c= 0.32	P	P	P	P
N5	Portland cement concrete (control), w/c= 0.43	M	P	P	P
N6	Portland cement concrete (control), w/c= 0.55	L	L	P	P
N4	Portland cement concrete (control), w/c= 0.76	M	L	L	P

Note: P = Passive; L = Low; M = Moderate; and H = High.

Table 9(c)—Severity of corrosion after 6 months evaluated by AC impedance technique

No.	Concrete mixture	13mm	25mm	51mm	76mm
N7	Concrete incorporating 10% silica fume, w/(c+sf) = 0.32	P	P	P	P
N8	Concrete incorporating 55% slag, w/(c+s) = 0.32	L	P	P	P
N3	Portland cement concrete (control), w/c= 0.32	P	P	P	P
N5	Portland cement concrete (control), w/c= 0.43	H	P	P	P
N6	Portland cement concrete (control), w/c= 0.55	H	H	P	P
N4	Portland cement concrete (control), w/c= 0.76	H	L	L	P

Note: P = Passive; L = Low; M = Moderate; and H = High.

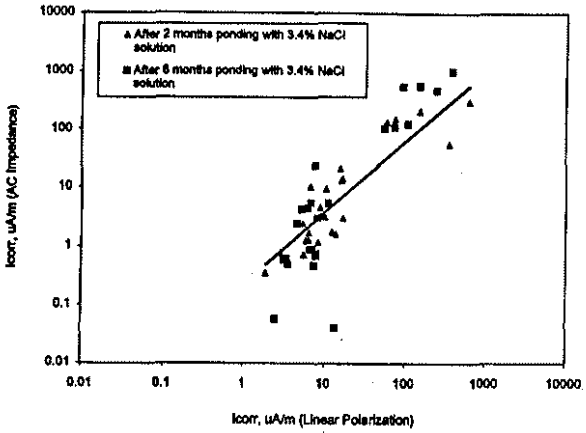

Fig. 7—Log-log plot on I_{corr} values obtained by both linear polarization and AC impedance techniques.

cover can significantly influence the rate of carbonation and the diffusion of corrosion-inducing species into the concrete-steel interface region. The thicker this cover is, the longer it takes for the chloride ions to reach the surface of reinforcing steel. A greater protection against corrosion is therefore assured.

The corrosion conditions of the steel reinforcement in the six reinforced concrete slabs were evaluated after 6 months of chloride ponding. Table 9(a) summarizes the corrosion probability of steel reinforcements by means of half-cell potential according to ASTM Standard C 876-91. The silica fume concrete and the control concrete with a w/c of 0.32 showed no probability of corrosion, even on the steel-reinforcing bars with 13 mm concrete cover. The steel reinforcements in slag concrete also showed low probability of corrosion, except for one bar with 13 mm concrete cover. In contrast, for all other control concretes with $w/c \geq 0.43$, the first two reinforcing steel bars with 13 mm cover depicted a high probability of corrosion. For concrete with a w/c of 0.76, even the reinforcing bars with 25 mm cover showed a high probability of corrosion.

Tables 9(b) and 9(c) give a summary of the corrosion conditions of the steel reinforcement in the six concrete slabs evaluated by the linear polarization and the AC impedance techniques, respectively. It is clear that the silica fume, slag, and control concretes with w/cm of 0.32 provide adequate tion to the reinforcing steel from corrosion in terms of mitigating the chloride ion penetration. At a depth of 13 mm, however, there was an indication of a low level of corrosion activity for the steel bars in the slag concrete. As expected, the poorest performance of the reinforcing bars was in the control concrete with a w/c of 0.76, where corrosion of the reinforcing steel was detected even with 51 mm concrete cover. Significant corrosion of reinforcing steel was also found in the control concrete slabs with a w/c of 0.43 at a 13 mm depth after 6 months of ponding with the chloride solution. A similar corrosion condition of the reinforcing bars with 13 and 25 mm covers was also observed in the slab with a w/c of 0.55, and the corrosion rates of these reinforcing bars obtained by the AC impedance technique were much higher than those obtained by the linear polarization technique. Such differences might be due to the polarization behavior of these two techniques and errors introduced during the data analysis. Regardless of the difference, the results confirmed the evaluation by the half-cell potential measurement.

The results of the resistance to chloride ion penetration determined according to ASTM C 1202 indicated that the slag concrete would have better resistance to chloride ion penetration than all the control portland cement concrete mixtures. The half-cell potential and the corrosion current measured by the linear polarization and the AC impedance techniques, however, indicated that the slag concrete did not provide as good protection to the reinforcing bars with 13 mm cover as the control portland cement concrete with a w/c of 0.32. The previous discrepancy in the test results may be attributed to the nature of the tests, and the fact that the specimens for ASTM C 1202 were moist cured for 28 days, whereas the specimens for the other tests were moist-cured for 7 days, followed by curing in the laboratory air for about 50 days. The relatively poor performance of the reinforcing bars embedded in the slag concrete with 13 mm cover might be due to the slight segregation of the slag cover concrete, and the relatively short duration of moist curing.

CONCLUDING REMARKS

1. Both the silica fume and slag concretes exhibited very low penetrability to chloride ions, with the value of the charge passed being less than 1000 coulombs (ASTM C 1202). All the control concretes had the value of charge passed greater than 1000 coulombs, regardless of the w/c;

2. The corrosion of steel reinforcing bars as determined by the half-cell potential, the linear polarization, and the AC impedance techniques indicated that, regardless of the thickness of concrete cover, there was no significant corrosion of the reinforcing steel in the silica fume, slag, and control concrete with a w/cm of 0.32 after 6 months of ponding with a 3.4% sodium chloride solution; and

3. Significant corrosion rates were observed for the reinforcing steel embedded in the control portland cement concrete with $w/c \geq 0.43$. As expected, the poorest performance was of the control concrete with a w/c of 0.76, where the corrosion of reinforcing steel was detected, even with 51 mm concrete cover.

ACKNOWLEDGMENTS

Grateful acknowledgement is made to Electric Power Research Institute (EPRI) of Palo Alto, Calif. for funding of the project. Thanks are due to Nathalie Chagnon, Bruce Baldock, Glendon Pye and Bob Myers of NRC/IRC, and R. Chevrier and A. Ferro of CANMET for their help with the experimental work.

REFERENCES

1. Malhotra, V. M., and Mehta P. K., "Pozzolanic and Cementitious Materials," *Advance in Concrete Technology*, V.1, Gordon and Breach Publishers, Canada, 1996.

2. Malhotra, V. M., "Role of Supplementary Cementing Materials in Reducing Greenhouse Gas Emissions," CANMET *Report* MTL 98-03 (OP&J), Mar. 1998. 16 pp.

3. Page, C. L.; Short, N. R.; and Holden, W. R., "Influence of Different Cement on Chloride Induced Corrosion of Reinforcing Steel," *Cement and Concrete Journal*, V. 16, 1986, pp. 79-86.

4. Byfors, K., "Influence of Silica Fume and Fly Ash on Chloride Diffusion and pH Values in Cement Paste," *Cement and Concrete Journal*, V. 17, 1987, pp. 115-130.

5. Mangat, P. S., and Molloy, B. T., "Influence pfa, Slag and Microsilica on Chloride Induced Corrosion of Reinforcement in Concrete," *Cement and Concrete Journal*, V. 21, 1991, pp. 819-834.

6. Kumar, A., and Roy, D. M., "Pore Structure and Ion Diffusion in Admixture Blended Portland Cement Systems," *Proceedings*, 8th International Conference on the Chemistry of Cement, V. IV, Rio de Janeiro, 1986, pp. 73-79.

7. Page, C. L., and Vennesland, O., "Pore Solution Composition and Chloride Binding Capacity of Silica Fume Cement Pastes," *Materials and Structures*, V. 16, No. 91, 1983, pp. 19-25.

8. Berke, N. S., "Resistance of Microsilica Concrete to Steel Corrosion, Erosion, and Chemical Attack," *Proceedings of the International Conference on Fly Ash, Silica Fume, Slag and Natural Pozzolans in Concrete*, SP-114, V. M. Malhotra, ed., American Concrete Institute, Farmington Hills, Mich., 1989, pp. 861-886.

9. EG&G, Princeton Applied Research Application Note-140, "Linear Polarization," and Note-148, "Tafel Plot."

10. John, D. G.; Searson, P. C.; and Dawson, J. L., "Use of AC Impedance